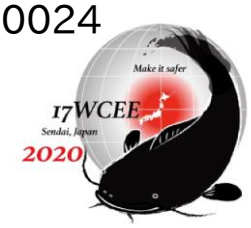

17th World Conference on Earthquake Engineering, 17WCEE
Sendai, Japan - September 13th to 18th 2020

Verification on Accumulating of Roughend Concrete and Post-Installed Anchor in Seismic Reinforcement Joints

Y. Okuyama[(1)], T. Yamada[(2)] , Y. Takase[(3)], T. Abe[(4)], K. Sakamoto[(5)], T. Hiwatashi[(6)]

[(1)] Graduate Student, Division of Sustainable and Environmental Engineering, Muroran Institute of Technology, 19041017@mmm.muroran- it.ac.jp
[(2)] Graduate Student, Division of Sustainable and Environmental Engineering, Muroran Institute of Technology, 16021111@mmm.muroran- it.ac.jp
[(3)] Associate Professor, College of Design and Manufacture Technology, Muroran Institute of Technology, y.takase@mmm.muroran- it.ac.jp
[(4)] Chief, Seismic Solution Department, TOBISHIMA Corporation, Takahide_Abe@tobishima.co.jp
[(5)] Chief, Seismic Solution Department, TOBISHIMA Corporation, Keita_Sakamoto@tobishima.co.jp
[(6)] Senior Researcher, Research and Develop Center, TOA Corporation, t_hiwatashi@toa-const.co.jp

Abstract

In recent years, existing concrete structures that do not satisfy seismic design standards are being reinforced by adding new strengthening members. These additional members are attached to the sides of existing members using post-installed anchors and roughening the concrete surface. Previous studies have not discussed in detail the combined mechanical behaviors of post-installed anchors and roughened concrete surfaces. Hence, the current design guidelines only consider the shear capacity of a post-installed anchor. Here, we believe that the mechanical behaviors of post-installed anchors and roughened concrete can be expressed by the Dowel and interlocking action, respectively. Additionally, in the authors' previous studies, the mechanical behavior of the roughened concrete was simply modeled as a trilinear model based on the shear loading test results of the roughened concrete surface. Then, the authors additionally conducted the shear loading tests in which the roughened area ratio, the maximum depth and the strength of existing concrete were as the test parameters. Subsequently, based on the constitutive law of the cracked concrete surface and considering the friction of the local uneven surface, a mechanical model of the roughening surface, for a bearing failure mode, was constructed. However, as described above, post-installed anchors as well as roughened concrete surfaces are used to reinforce joints. Therefore, the combined model, which included the Dowel and roughened concrete model, was investigated. This was done because the mechanism of the joint surface may change when the anchors as well as the roughened concrete surface is applied. In this paper, the specimens with post-installed anchors and roughened concrete, were tested, and the verification was conducted by the combined model. By modifying the function of the opening behavior, position of the plastic hinge point, and contact stress model, it is possible to evaluate the experimental results when both the reinforcements are applied. It was also found that the test results could be estimated with reasonable accuracy even when the axial stress and anchor diameter varied.

Keywords: Seismic retrofitting, Roughened concrete, Shear stress transfer, Post-installed anchor

1. Introduction

Seismic strengthening of existing buildings is imperative in Japan, due to the frequent occurrence of strong earthquakes. In seismically strengthened structures, the extension members of structures are generally connected to existing members using post-installed anchors and roughened concrete. In Japan, concrete surfaces are roughened using an electric hammer (chipping). Shear stress is transferred by contact in the local unevenness on roughened concrete. In the current design guidelines[1], only the shear strength of post-installed anchors is considered. Research that combines the shear strength of both post-installed anchors and roughened concrete is scarce, based on the literature review conducted for this study. Therefore, a mechanical model of the roughened concrete is proposed in this study. This is achieved by using the Bujadaham model[2] (which considers contact stress) for the transfer mechanism of shear stress in cracked concrete. Subsequently, the stress of the joint can be estimated by combining this mechanical model of roughened concrete with a dowel model containing post-installed anchors. Shear loading tests of joints using roughened concrete and post-installed anchors are conducted in this research, and the adaptability of the model to test results is investigated.

2. Outline of Mechanical Model

In this research, the overall shear force acting on the joint surface q_j is calculated as the combined resistance by the dowel model of a post-installed anchor q_a (which was constructed in a previous research study), and the shear force resisted by the roughened concrete q_{cr}. The adaptability of the model with the test results is investigated.

$$q_j = q_a + q_{cr} \tag{1}$$

In this section, the outlines of q_a and q_{cr} are explained.

2.1 Dowel model of post-installed anchor

The dowel model[3] of the post-installed anchor is briefly summarized in this study. A detailed discussion of this model can be found in prior research[2].

The dowel model used in this study is idealized as shown in Figure 1, so that the mechanical behavior in the non-linear region can be easily reproduced. Additionally, Figure 2 shows the elongation and tensile stress generated in the axial direction of the anchor bars. When a shear force is applied on the joint surface, the anchor bars deform, and a plastic hinge is formed. Therefore, a bearing stress σ_b is generated in the concrete, and a tensile stress σ_{br} acts and an apparent shear force is applied when the anchor bars extend axially. Therefore, the shear force q_a carried by the anchor bars is the bending resistance q_S at the plastic hinge point, and the bearing resistance q_B acting on the concrete is the shear component q_T^S of the tensile force of the reinforcing bar acting axially.

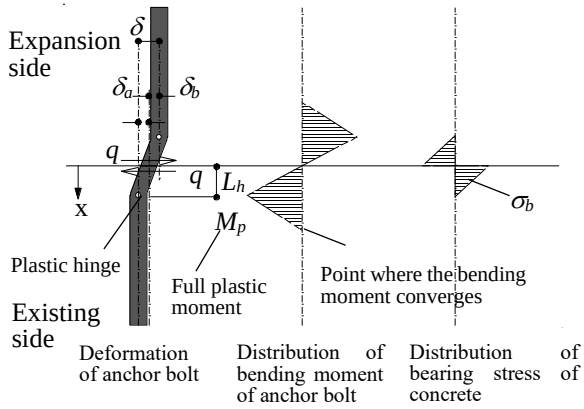

Fig.1 Dowel model of post installed anchor

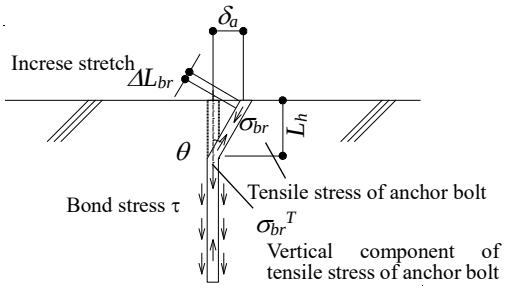

Fig.2 Anchor-bolt stretches with increasing the shear displacement

Figure 3 shows the composition model of q_S and q_B. The bearing resistance is assumed to act on the half circumference of the anchor in the loading direction, and q_B can be obtained by Equation (2). q_T is a tensile force that acts in the axial direction of the anchor muscle. The shear of this force is q_T^S as shownEquation (3). The mechanical model of q_T is a bilinear model expressed by Equation (4).

$$q_B = \frac{\pi\phi}{2}\int_0^{L_h}\sigma_b(x)dx \tag{2}$$

$$q_T^S = q_T \sin\theta = \sigma_{br}\frac{\pi\phi^2}{4}\sin\theta \tag{3}$$

$$\sigma_{br} = \begin{cases} E_S \cdot \varepsilon_{br} & (\varepsilon_{br} < \varepsilon_y) \\ \sigma_y & (\varepsilon_y \le \varepsilon_{br}) \end{cases} \tag{4}$$

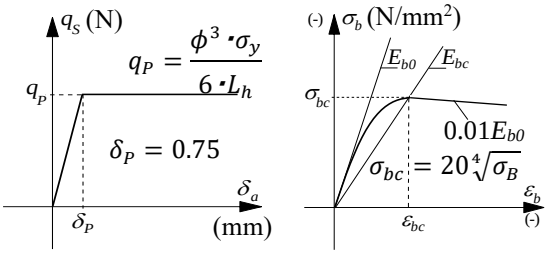

(a) Bending resistance of plastic hinges (b) Bearing resistance of concrete

Fig.3 Mechanical model of structural materials

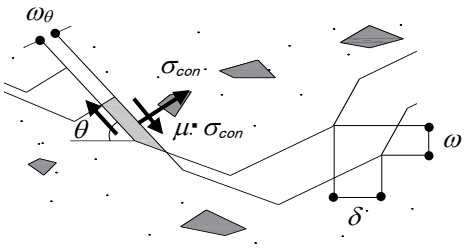

Fig.4 Conceptual diagram of contact stress acting on micro uneven surface

Here, σ_{br} and ε_{br} are the tensile stress and strain acting on the anchor, ε_y is the yield strain of the anchor, and E_S is the Young's modulus.

2.2 Mechanics model of concrete roughened concrete surface

The outline of the mechanical model of the concrete roughened surface used in this research is referred to as the "roughened concrete model"[4,5], described as follows:

Figure 4 represents a conceptual diagram[4] of the contact stress acting on the uneven local surface. The roughened concrete model is constructed based on the Bujadaham model[2], which is a model for shear stress transfer of cracked concrete. The contact stress σ_{con} and the frictional stress ($\mu \times \sigma_{con}$) are generated when the uneven micro surfaces come in contact with each other. The shear stress τ_{cr} and the vertical stress σ_{cr} can be calculated by separating the horizontal and vertical components, multiplying it with the contact area effective rate K and the angle density function $\Omega(\theta)$, and integrating it with $d\theta$, as shown in Figure 4. It is expressed in Equation (5) based on Figure 4.

$$\tau_{cr} = \int_{-\pi/2}^{\pi/2} K \cdot \sigma_{con} \cdot \Omega(\theta) \cdot (\sin\theta + \mu\cos\theta)d\theta \tag{5}$$

$$\sigma_{cr} = \int_{-\pi/2}^{\pi/2} K \cdot \sigma_{con} \cdot \Omega(\theta) \cdot (\cos\theta - \mu\sin\theta)d\theta \tag{6}$$

where θ is the inclination angle of the local surface, and μ is the friction coefficient. Because the contact of the local uneven surface occurs on flat surfaces, the value of μ = 0.6, according to the guidelines of precast reinforced concrete structure[4]. A shape analysis of the roughened model surface is performed using a laser displacement meter, and the inclination angle of the micro uneven surface is obtained by measuring its three-dimensional coordinate data. The angle density is calculated by using the three-dimensional coordinate data acquired from the shape measurement experiment. The following equation is used to simulate the angle density distribution[4].

$$\Omega(\theta) = \frac{4}{3}(a_0 + a_1 \cdot |\theta|^n) \cdot cos^m\theta \tag{7}$$

where a_0, a_1, n, and m are coefficients that represent angle density functions for each rough surface area ratio r_{cr}, set by the least square method so that the angle density distribution of the rough surface can be simulated. Table 1 shows the values of these coefficients. Figure 5 shows the modeling of the contact direct stress of the micro uneven surface.

Table1 Parameters of angle density function

r_{cr}	Parameters			
	a_0	a_1	n	m
0.10	1.22	-1.11	0.44	3.09
0.20	1.16	-1.05	0.43	2.54
0.30	1.12	-0.99	0.41	2.10

r_{cr}: Area ratio of roughened concrete surface

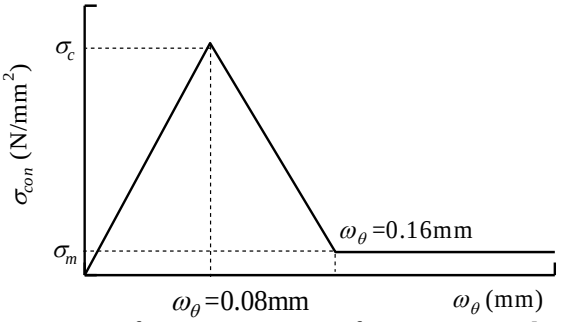

Fig.5 Contact stress of micro uneven surface - Contact displacement relation

3. Outline of Experiment

3.1 Specimen parameters

Table2 shows the parameters of the specimens. The test parameters are r_{cr} , with or without anchor bars, and the average compressive stress σ_0 (hereinafter referred to as "axial stress") generated in the joint surface. r_{cr} is assumed to be three levels of 0.1, 0.2 and 0.3, and the target σ_B is 20 N /mm^2. The anchor muscle diameter is 13mm and 16mm. Test specimen names are consisted by the symbols (A: post-installed anchor, R: roughened concrete, AR:both), numerical value for r_{cr}, and axial stress (LM:0.48N/mm^2, MM:0.95N/mm^2). In the previous experiments, the axial stress was set to 0.48 N/mm^2, but in this paper, 0.95N/mm^2, which is twice value, was newly set. Table3 shows the material properties of concrete, grout and anchor bars respectively.

3.2 Specimens shape and construction method

Figure 6 shows the dimensions of the specimen. The test area shall be 375 mm × 200 mm of the concrete on the existing member side. The roughened surface is constructed using a vibration hammer and r_{cr} is confirmed using image analysis. Double-place the post-installed anchor of the ϕ 16 (σ_y: 369 N/mm^2) and Single-place the post-installed anchor of the ϕ 13 (σ_y: 403 N/mm^2). The effective implantation depth of the anchor muscle was 7*da* (*da*: diameter of anchor muscle). The grout is a premix type. To grasps the shear resistance performance of a pure roughened part, so grease is applied in advance to the smooth part without the uneven parts, and the influence of friction and adhesion was reduced. Strain gauges are attached to the anchor bars at depths of 0.5*da*, 2*da* and 5*da* on the existing member side and heights of 0.5*da* and 2*da* on the extension member side.

Table2 Test parameters

Test body name	r_{cr}	r_{cr} Measured value	σ_0 (N/mm^2)	ϕ (mm)
R-10LM	0.10	0.099	0.48	–
R-20LM	0.20	0.213		
R-30LM	0.30	0.290		
A1-16-0LM	–	–		16
AR2-16-10LM	0.10	0.117		
AR2-16-20LM	0.20	0.204		
AR2-16-30LM	0.30	0.301		
AR2-16-10MM	0.10	0.104	0.95	
AR2-16-20MM	0.20	0.195		
AR2-16-30MM	0.30	0.293		
AR1-16-10LM	0.10	0.093	0.48	
AR1-13-10LM	0.10	0.108		13
AR1-13-20LM	0.20	0.210		
AR1-13-30LM	0.30	0.316		
A1-13-0LM	–	–		

ϕ: Anchor muscle diameter σ_0: Axial stress

Table3 Material properties of specimens
(a) Concrete and grout

Test body name	Material	σ_B (N/mm^2)	Ec (kN/mm^2)	σ_t (N/mm)
R-10,30LM	Concrete	17.1	24.7	1.83
	Grout	64.6	26.2	2.10
R-20LM	Concrete	19.9	29.1	1.90
	Grout	68.7	26.3	3.42
A1-16-0LM	Concrete	21.2	21.8	2.09
	Grout	48.9	23.1	3.55
AR2-16-10,20,30LM	Concrete	21.1	26.3	–
	Grout	73.4	–	–
AR2-16-10,20,30MM	Concrete	20.8	27.3	2.30
A1-13-0LM	Grout	54.4	25.0	2.70
AR-1-16-10LM	Concrete	22.5	17.4	–
AR1-13-10,20,30LM	Grout	68.0	25.9	–

σ_B : Compressive strength Ec : Young's modulus σ_t : Split strength

(b) Anchor

Test body name	Diameter	Yield strengh (N/mm^2)	Young's modulus (kN/mm^2)
A1-16-0LM AR2-16-10,20,30LM AR2-16-10,20,30MM	ϕ 16	369	196
AR1-16-10LM		376	170
AR1-13-10,20,30LM	ϕ 13	403	174

3.3 Methods of loading and measuring

The loading equipment uses hydraulic jacks of 500 kN to control the axial stress and horizontal load of alternating positive and negative cycles. Shear force is applied under controlled displacement δ. A

displacement meter is installed on the existing concrete, and the distance (hereinafter referred to as the "opening amount ω") δ from the reference point attached to the extension member side are measured.

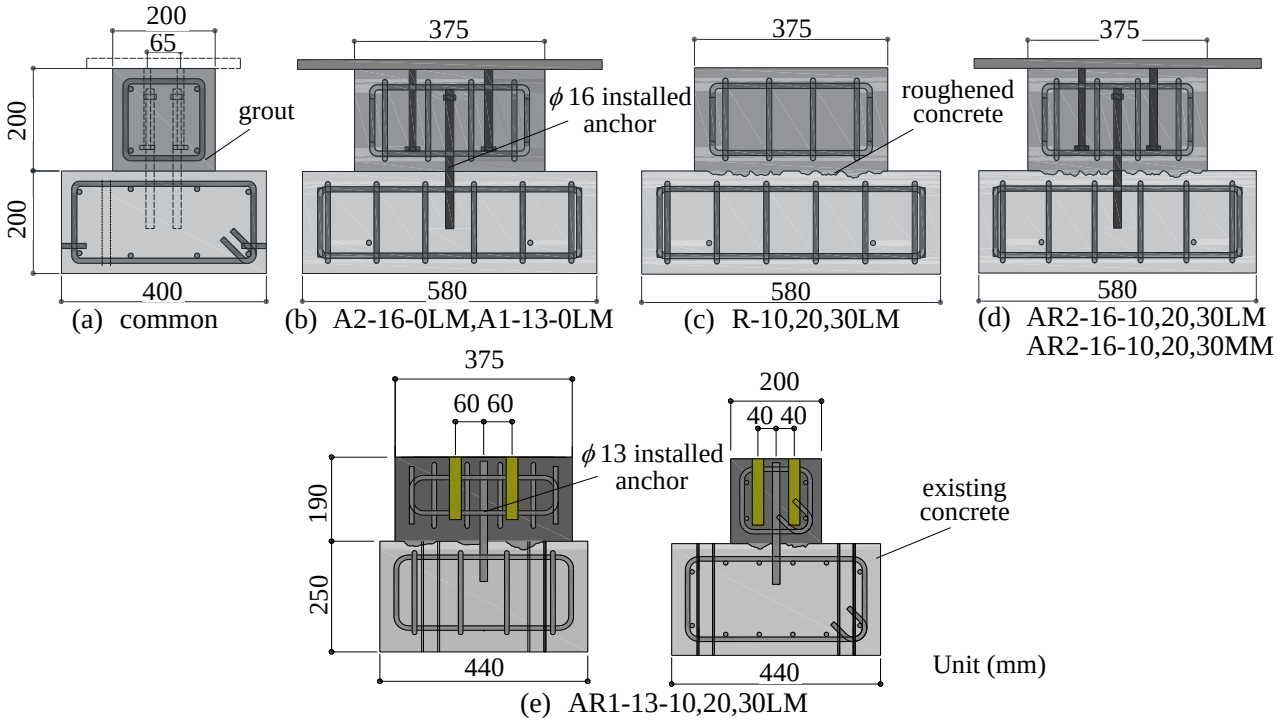

Fig.6 Dimension of specimen

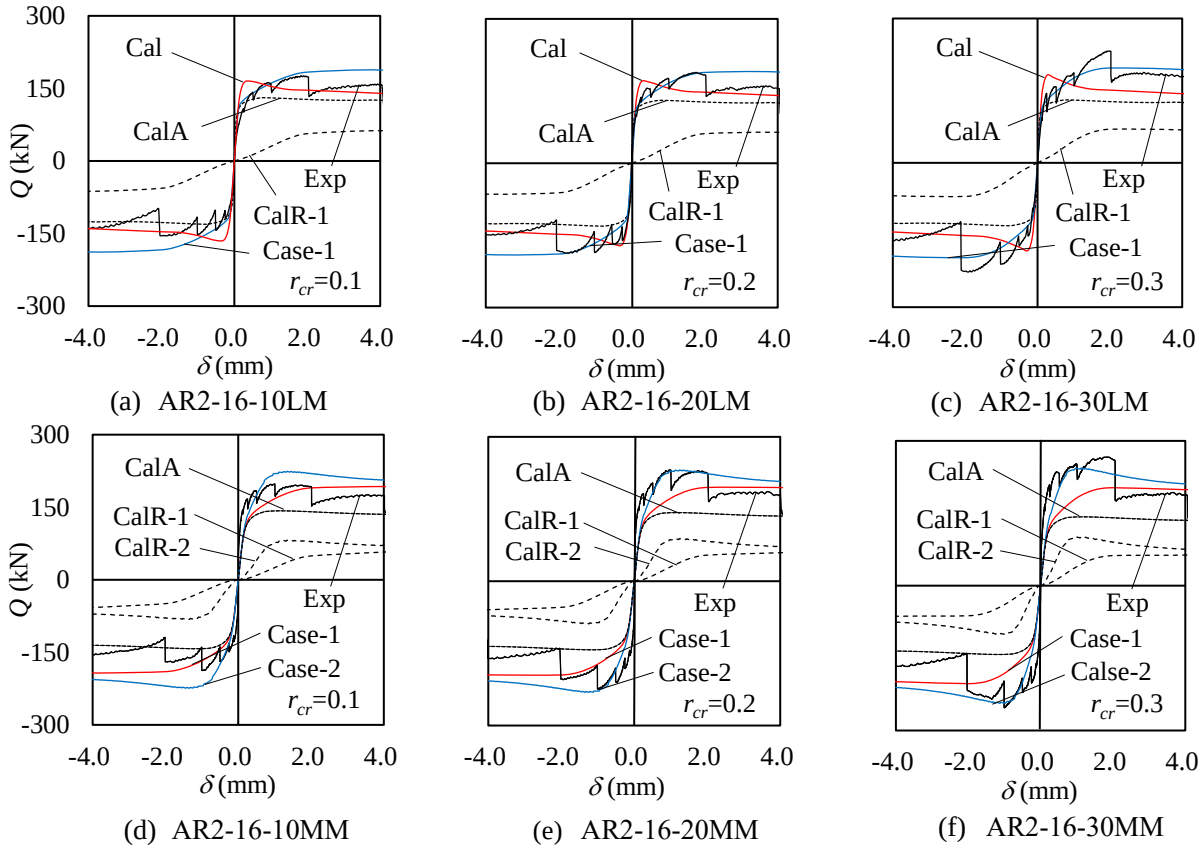

Fig.7 $Q-\delta$ relations of each specimen

4. Modification of Proposed Model

The first model considered was based on a ϕ16 anchor. Subsequently, an anchor of ϕ13 was used.

4.1 Test of ϕ16 anchor

Figure 7 shows the envelope (Exp) of the Q–δ relationship of each specimen. The experimental results show that the peak was reached at δ = 0.2–0.5 mm and a decrease in load was observed when only roughened concrete[3,4] was used. However, when the roughened concrete and post-installed anchor were used in combination. There is a possibility that experimental results cannot be estimated by simply adding the current model. Therefore, in this section, experimental results are studied in detail, and modification to the outline model in Section [2] is made.

[1] Plastic hinge point and stress softening in concrete

Figure 8 shows the strain distributions in the anchor. AR2-16-10LM, 20LM, and 30LM tend to be deeper at the location where the strain becomes larger from the surface on the existing concrete side, compared to A16-0LM. Moreover, although there is a variation, the strain decreases as r_{cr} increases, and the strain of the test sample with only the anchor becomes the largest. In the dowel model, the position of the plastic hinge point shown in Figure 1 greatly affects all the calculation processes[2]. Therefore, the position of the plastic hinge point is set 1.5 times deeper than the previous model[2], based on the strain distribution, and is considered to be nearly consistent with the behavior confirmed in the experiment. Following this, the stress softening of concrete was investigated. From the experimental results, it was confirmed that the load gradually decreases after reaching the peak point when using both the roughened concrete and post-installed anchors. Therefore, the softening slope of the concrete shown in Figure 3 (b) is also modified to make it a gentler slope. In the current model, it is softened with a slope of 1% of the Young's modulus (=0.01E_{b0}); however, in the modified

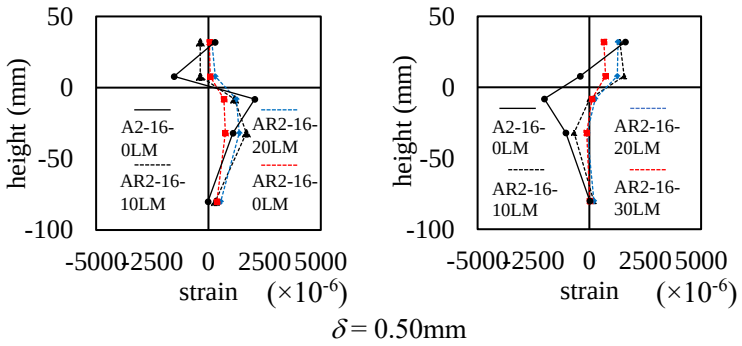

Fig.8 Strain distribution of anchor muscle

model, it is set to soften with a slope of 0.75% (=0.0075E_{b0}).

[2] Roughened concrete model

In previous research studies, experiments and modeling were conducted focusing on σ_0 = 0.48 N/mm^2. The model is modified based on this axial stress value, and subsequently re-modified based on the experimental result value of σ_0 = 0.95N/mm^2.

[2-1] Study based on σ_0 = 0.48 N / mm^2 (Case-1)

First, a quantitative evaluation of the opening amount ω is conducted. Figure 9 (a) shows the ω–δ relationship between R-10LM, 20LM, and 30LM and AR2-16-10LM, 20LM, and 30LM. When analyzed using the proposed model, the value of E obtained by regression analysis of the experimental ω–δ relationship is used. As shown in Figure 8, the behavior is different due to the residual strain of the anchor when used in combination with post installed anchors. Therefore, a regression analysis is performed on AR16-10LM, 20LM, 30LM, and a modified Equation (8) is derived.

$$\omega = 0.0087\delta^3 - 0.1046\delta^2 + 0.6144\delta \quad (8)$$

Subsequently, the contact model is considered. It can be theorized that the anchor bolts prevent failure around the roughened concrete for the joint with the both anchor bolts and roughened concrete. In this design mechanism, the contact displacement at the peak stress would be larger. Figure 10 shows a modified model (Case-1) of the contact stress of the uneven local surface. In the original model (Figure 5), the displacement at the peak was $\omega_{\theta c}$= 0.08 mm. However, in Case-1, $\omega_{\theta c}$ = 0.8 mm, based on the test results. Additionally, although the load decreases gradually (as observed in the experimental results), focusing on the behavior of each application cycle at the same displacement, the decrease in comparison with the virgin loading is large. Although this does not separate the existing part and the new part due to the anchor bars, it is presumed that the concrete itself is damaged in a brittle manner. Therefore, as shown in Figure 10, the brittle behavior was applied to Case-1. Because the load tends to converge to a constant value as displacement progresses in the Q–δ curve of each specimen, the contact stress of the micro uneven surface is also modeled to converge to a constant value.

[2-2] σ_0 = 0.95 N / mm^2 (Case-2)

Figure 9 (b) shows the relationship between AR2-16-10LM, 20LM, and 30LM and AR2-16-10MM, 20MM, and 30M. When the axial stress σ_0 is twice that of r_{cr} = 10%, the opening increases by approximately 20%; and when r_{cr} = 30% the opening increases by approximately 40%. However, for r_{cr} = 20%, the opening reduces by approximately 20%. Thus, no qualitative tendency can be observed from this experimental result. Therefore, a new regression analysis is performed including the specimen of σ_0 = 0.95 N/mm^2, and the following equation is introduced into the roughened concrete model.

$$\omega = 0.0028\delta^3 - 0.0655\delta^2 + 0.5613\delta + 0.0334 \quad (9)$$

Finally, the contact stress model is considered. The experimental results show that when the axial stress is twice the original stress, the peak position δ shifts to approximately 1.0 mm, which is about half that of the specimen with σ_0 = 0.48 N/mm^2. In addition, the maximum load increases by approximately 15% when compared with the same area ratio of the specimen. The contact stress model is modified based on this tendency. First, for a specimen with σ_0 = 0.95 N/mm^2, $\omega_{\theta c}$ is set to 0.4 mm (50% of 0.8 mm). As the axial stress increases, the opening decreases, and the contact displacement increases accordingly; therefore, σ_{con} increases. However, based on the results from the experiment, when the axial load was increased, ω did not always decrease. Therefore, the composition of the maximum contact stress σ_c is modified as represented in the following equation:

$$\sigma_c = 6.5\sqrt[3]{\sigma_B} \cdot \sigma_0 \quad (10)$$

The term "6.5 · $\sqrt[3]{(\sigma_B)}$" is similar to the formula proposed in Ref [4]. This effect is considered by multiplying it with σ_0 and is represented by Case-2 in Figure 10.

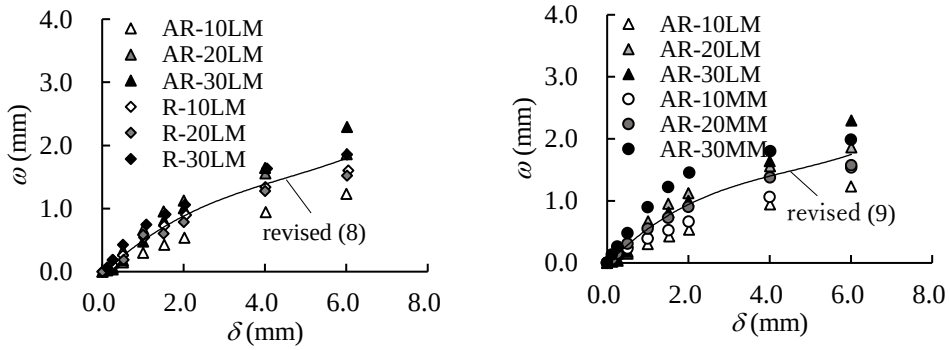

(a) Case-1 (b) Case-2

Fig.9 $\omega - \delta$ relationship

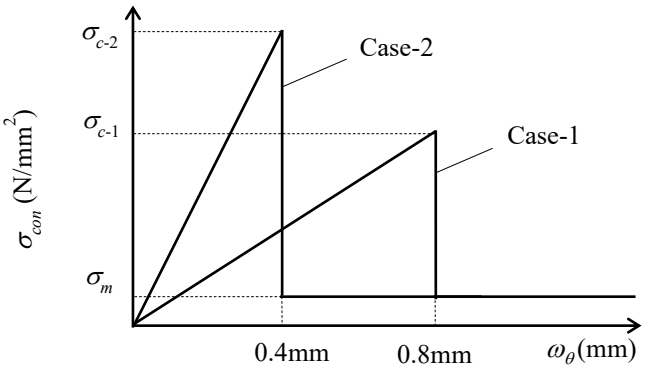

Fig.10 Contact direct stress

4.2 Adaptability of Modified Model to Experimental Results

The aforementioned Figure 7 (a), (b), and (c) show the pre-modified model (Cal) and the modified model (Case-1) of AR2-16-10LM, 20LM, and 30LM, the correction anchor model (CalA), and the modified roughened concrete model (CalR-1). In the pre-modified model, the deformation peaks at a small area of 1 mm or less behaves differently from the experiment. However, by the modified model, the test results can be accurately estimated. Table 4 shows a list of test results and analysis results on positive side loading. The experimental results can be traced with an accuracy of ±10% over the whole range of δ = 0.5 to 4.0 mm; however, focusing on δ = 2.0 mm, the model underestimated for AR-30LM by approximately 20%.

The modified models of Case-1 and Case-2 for AR2-16-10MM, 20MM, and 30MM are shown in Figures 7 (d), (e), and (f). Additionally, the modified roughened concrete models of Case-1 and Case-2 are shown as CalR-1 and CalR-2, respectively. The experimental results showed that the load gradually decreased after the peak in the case of σ_0 = 0.48 N/mm^2 was reached. However, in specimens AR2-16-10LM and 20LM, when σ_0 was increased, a smaller shift in the peak value was observed. Concurrently, it was observed that the maximum load increased with σ_0, in Case-1. These behaviors were deprecated; therefore, they could not be consistently reproduced. In Case-2, the experimental value can be evaluated within a range of ±20% with AR2-16-20MM and 30MM, but the experimental value is exaggerated with AR2-16-10MM.

4.3 Examination of anchor ϕ 13

In this research, the influence of the difference in anchor diameter was studied. This amount is considered the ratio of anchor bar to the roughened area ratio, and is referred to as the "rebar ratio/roughened ratio" (P_{ch}).

Figure 11 shows the model modification based on P_{ch}, Table 5 shows the model case, and Figure 12 shows the envelope (Exp) of the Q–δ relationship of each specimen. When the anchoring was reduced, the effect of

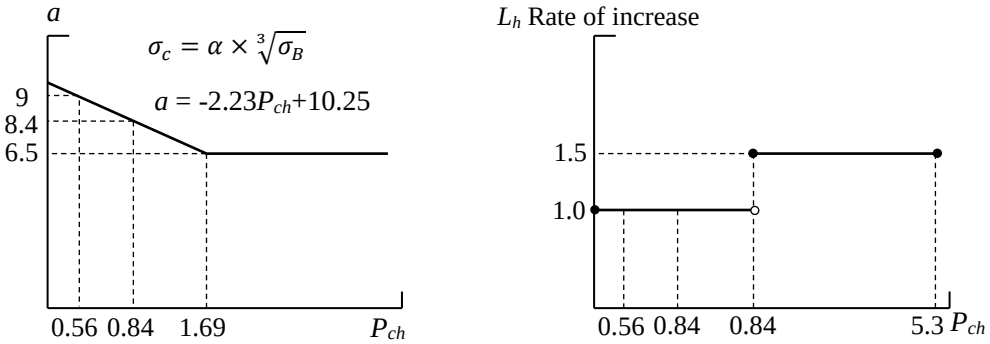

(a) a-P_{ch} Relationship (b) L_h Rate of increase -P_{ch} Relationship

Fig.11 $Q-\delta$ relation of each specimen

the roughened concrete was larger than the result of 2 (ϕ16). Therefore, three case models were developed: Case1 describes behavior closer to the anchor, Case3 describes behavior closer to the roughened concrete, and Case 2 describes the middle.

[1] Examination of contact stress model

Figure 13 shows a contact stress model. For this model, the maximum contact stress is calculated by the following equation:

$$\sigma_c = \alpha \times \sqrt[3]{\sigma_B} \tag{11}$$

For the specimens with small P_{ch}, $\alpha = 9$, and for specimens with large P_{ch}, $\alpha = 6.5$. If the maximum contact stress is proportional to P_{ch}, α is expressed by the following equation:

$$\alpha = -2.23P_{ch} + 10.25 \ (0 \le P_{ch} < 1.69) \tag{12}$$

Substituting P_{ch} = 0.84 for AR1-13-20LM into this equation results in α = 8.4. Therefore, as shown in Table 5 and Figure 13, this study considers three stages of α, at values of 6.5, 8.4, and 9.0. In addition, the behavior of the post-peak region is different from that of the double bar arrangement using a single anchor.

Table5 Model Case

Analysis number	$\omega_{\theta c}$	σ_c=α*$\sqrt[3]{\sigma_B}$	L_h Rate of increase
Case1	0.16	6.5*$\sqrt[3]{\sigma_B}$	1.5times
Case2	0.16	8.4*$\sqrt[3]{\sigma_B}$	1.0 times
Case3	0.16	9*$\sqrt[3]{\sigma_B}$	1.0 times

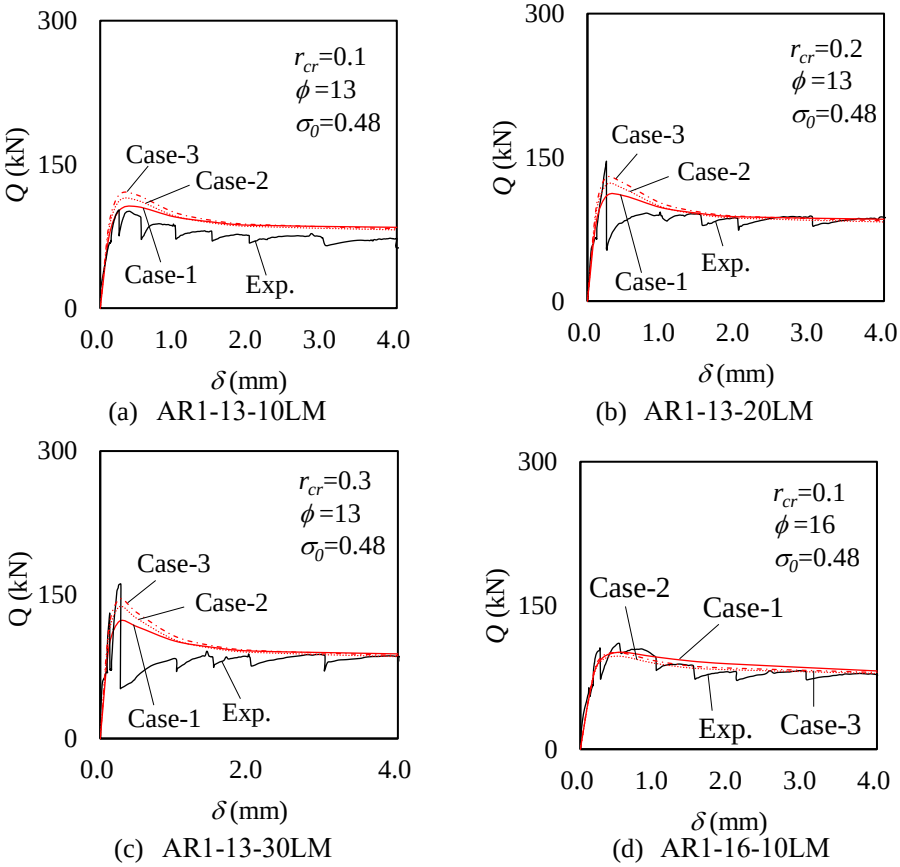

Fig.12 $Q-\delta$ relation of each specimen

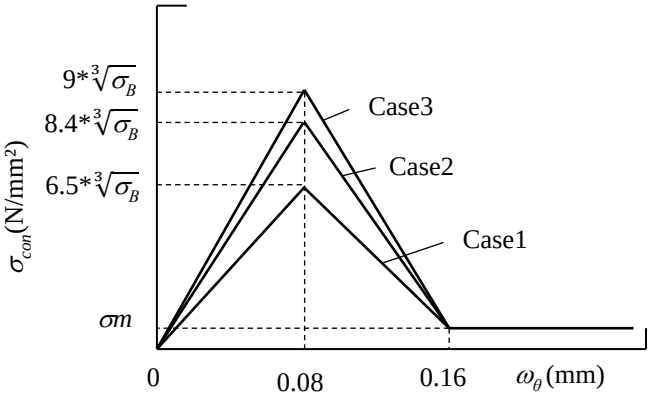

Fig.13 Contact direct stress

[2] Plastic hinge point

As mentioned in the previous section, the value of P confirmed that the behavior was closer to the anchor, closer to the rough surface, and intermediate between them. Therefore, when P_{ch} is large, the position is set to be 1.5 times deeper, and when P_{ch} is small, the position is the same as the anchor.

[3] Opening behavior

Figure 15 shows the ω–δ relationship among AR1-13-10LM, 20LM, and 30LM. A new regression analysis is conducted on AR1-13-10LM, 20LM, and 30LM and the following equation is derived:.

$$\omega = 0.0024\delta^3 - 0.0519\delta^2 + 0.4557\delta \tag{13}$$

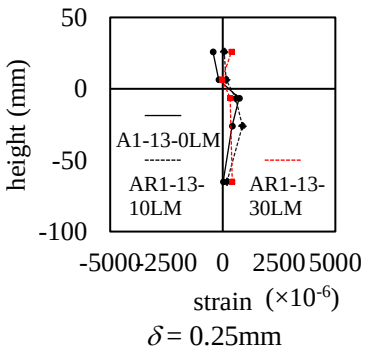

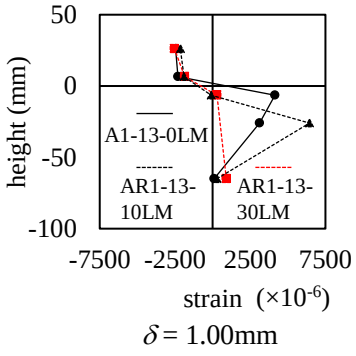

Fig.14 Strain distribution of anchor muscle

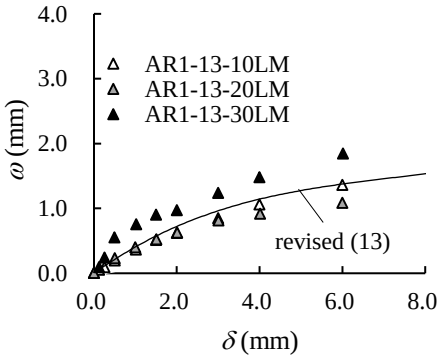

Fig.15 $\omega - \delta$ relationship

4.4 Adaptability of modified model to experimental results

[1] When P_{ch} is large

For AR1-13-10LM and AR1-16-10LM shown in Figures 12 (a) and (d), when P_{ch} is large, the tendency of the anchor is strong. Therefore, the behavior of roughening is dominant. Case 2 and Case 3 overestimate the experimental results over the entire displacement. Conversely, for Case 1, the maximum load underestimates the experimental results. However, after δ = 1.0 mm, the experimental results can be reproduced. Thus, Case1 is recommended for these specimens.

[2] When P_{ch} is small

For AR1-13-20LM and AR1-13-30LM in Figures 12 (b) and (c), when P_{ch} is small, it becomes more susceptible to roughening. Based on these figures, the maximum load of Case 1 is the smallest, and Case 2 and

Case 3 have higher suitability. Therefore, it is recommended that these specimens be modified accordingly, so that the roughening behavior becomes more pronounced.

5. Conclusion

In this study, shear loading tests were performed on specimens using post-installed anchors and roughened concrete at seismically reinforced joints. These were verified with a mechanical model for evaluating the shear load-displacement relationship. By modifying the amount of opening, the position of the plastic hinge point, the concrete softening coefficient, and the contact stress model, the experimental result in the case of $\sigma_0 = 0.48$ N/mm^2 could be reasonably estimated. Additionally, even if the axial stress was doubled, it was possible to capture the general shape by correcting the gap and contact stress model.

In the experiment with different anchor diameters, a new study item called “the roughening rebar ratio” was added and the model was modified. Therefore, the modified model was a good match to the experimental results for $\phi = 13$ mm and $\sigma_0 = 0.48$ N/mm^2.

In the future, we will continue to verify the detailed mechanisms such as double reinforcement of ϕ 13 and parameter increase with a different diameter of reinforcing bars.

6. References

[1] Japan Building Disaster Prevention Association: Revised version 2017 Revised edition Guideline and commentary on retrofitting of existing reinforced concrete buildings, Japan Building Disaster Prevention Association, 2017 (2017 revised edition 2nd print)

[2] Bujadaham Buja: The Universal Model for Transfer across Crack in Concrete Department of Civil Engineering The Graduate School of The University of Tokyo，1991.3

[3] Takase Yuya, Wada Toshiyoshi, Ikeda Takaaki, Shinohara Yasuji: Mechanic model of post installed anchors subjected to repeated shear force, Proceedings of the Architectural Institute of Japan 77, 682, pp. 1915-1924, 2012.12

[4] Isozaki Tsubasa, Takase Yuya, Abe Takahide, Katori Keiichi: Basic research on shear resistance of concrete roughened in existing members, Proceedings of the Japan Concrete Institute, Vol.39, No1, pp. 919-924, 2017.6

[5] Isozaki Tsubasa, Takase Yuya, Abe Takahide, Sakamoto Keita, Hiwatashi Ken, Katori Keiichi: A Constitutive Model Reproducing Shear Stress Transfer Mechanism of Concrete Roughened with Different Compressive Strength, Concrete Engineering Annual Report, Vol.40, No2, pp. 73-78, 2018.6

